

Article

Synthesis, Photochemical and In Vitro Cytotoxic Evaluation of New Iodinated Aminosquaraines as Potential Sensitizers for Photodynamic Therapy

Filipa Mandim ^{1,2}, Vânia C. Graça ¹, Ricardo C. Calhella ², Isabel L. F. Machado ^{3,4},
Luis F. V. Ferreira ³, Isabel C. F. R. Ferreira ^{2,*} and Paulo F. Santos ^{1,*}

- ¹ Centro de Química-Vila Real (CQ-VR), Universidade de Trás-os-Montes e Alto Douro, 5001-801 Vila Real, Portugal; filipamandim@ipb.pt (F.M.); vcsgg_22@hotmail.com (V.C.G.)
- ² Centro de Investigação de Montanha (CIMO), Instituto Politécnico de Bragança, Campus de Santa Apolónia, 5300-253 Bragança, Portugal; calhella@ipb.pt
- ³ CQFM-Centro de Química-Física Molecular and IN-Institute for Nanosciences and Nanotechnologies and IBB-Institute for Bioengineering and Biosciences, Instituto Superior Técnico, Universidade de Lisboa, 1049-001 Lisboa, Portugal; ilferreiramachado@tecnico.ulisboa.pt (I.L.F.M.); LuisFilipeVF@ist.utl.pt (L.F.V.F.)
- ⁴ Instituto Politécnico de Portalegre, P-7300-110 Portalegre, Portugal
- * Correspondence: iferreira@ipb.pt (I.C.F.R.F.); psantos@utad.pt (P.F.S.);
Tel.: +351-273-303-219 (I.C.F.R.F.); +351-259-350-321 (P.F.S.)

Received: 6 January 2019; Accepted: 23 February 2019; Published: 28 February 2019



Abstract: In this work, several benzothiazole-based aminosquaraine dyes, displaying strong absorption within the so-called phototherapeutic window (650–800 nm), were synthesized. The ability, of all the new dyes, to generate singlet oxygen was assessed by determining the correspondent phosphorescence emission and through the comparison with a standard. The quantum yields of singlet oxygen generation were determined and exhibited to be strongly dependent on the nature of the amino substituents introduced in the squaric ring. The photodynamic activity of the synthesized dyes was tested against four human tumor cell lines: breast (MCF-7), lung (NCI-H460), cervical (HeLa) and hepatocellular (HepG2) carcinomas; and a non-tumor porcine liver primary cell culture (PLP2). All the compounds synthesized were found to be able to inhibit tumor cells growth upon irradiation more than in the dark, in most of the cases, very significantly. Considering the photodynamic activity exhibited and the low toxicity displayed for the non-tumor cells, some of the synthesized dyes can be regarded as potential candidates as photosensitizers for PDT.

Keywords: squaraine; singlet oxygen; photodynamic therapy

1. Introduction

Photodynamic therapy (PDT) has emerged as a very promising treatment for certain types of cancer and other non-oncologic disorders [1]. Over the years, PDT has received regulatory approval worldwide for several conditions and has now become an established therapeutic modality [2].

The basic principle underlying this therapeutic approach is simple: a light-absorbing molecule, after being administrated to the patient, is activated with light of an appropriate wavelength and gives rise to the production of reactive oxygen species (ROS). This species are responsible to induce damage of the surrounding cells [3]. Following interaction with light, the sensitizer, which is firstly excited to its excited singlet state, may efficiently populate, via intersystem crossing, the longer-lived excited triplet state. The triplet state of the sensitizer can then produce ROS by two different competing mechanisms [4]. In a Type I reaction, the sensitizer in the triplet state can react with organic substrates or solvents to generate free radicals that subsequently interact with oxygen to generate ROS such

as superoxide radical anion and hydroxyl radical. Alternatively, it can transfer its energy directly to surrounding ground-state triplet oxygen to produce highly cytotoxic singlet state oxygen in a process called Type II reaction.

Both Type I and Type II reactions can occur in parallel. Their relative contribution depending chiefly on the nature of the sensitizer and the concentration of oxygen [5]. However, singlet oxygen, which acts catalytically, is generally considered to be the main cytotoxic agent responsible for the photodynamic effect [6]. Independently of the nature of the ROS generated during the photodynamic process, the ultimate outcome is the cell destruction, which can occur by three main mechanisms: direct cell death, either by apoptosis, necrosis or autophagy [7], vascular collapse and ensuing tissue hypoxia [8], and activation of inflammatory and immune responses [9]. Because the photodynamic process only takes place when the photosensitizer, oxygen and light are present simultaneously, PDT comes to be a particularly selective modality, with unique advantages compared to conventional tumor therapies such as surgery, chemotherapy and radiotherapy [10,11].

Photofrin[®], a mixture of hematoporphyrin derivatives, was the first photosensitizer to receive regulatory approval in several countries for the treatment of various cancers. After more than twenty years is still the most frequently used PDT sensitizer in clinical practice [12]. Despite its popularity, Photofrin[®] has several disadvantages, including chemical inhomogeneity, prolonged skin photosensitivity, low absorption of light and poor tissue penetration of light [13]. These drawbacks impelled a large research effort towards the development of new molecules that could meet the main requirements of an ideal sensitizer. Amongst these are [14]: (i) to be a single chemical entity; (ii) minimal dark toxicity and cytotoxicity only upon illumination; (iii) rapid clearance from the body to provide low systemic toxicity; (iv) high triplet quantum yield to efficiently generate ROS, namely singlet oxygen, upon irradiation; (v) strong absorption in the phototherapeutic window (650–800 nm), where the depth of light penetration in tissue is maximal, to allow the use of low drug dosages.

While no ideal photosensitizer has yet been discovered, a number of the so-called second generation photosensitizers have been developed, either porphyrin-based or non-porphyrin compounds, a small number of which have already granted regulatory approval for clinical oncotherapy while some of others are currently under clinical trials [12,15–17].

Squaraine dyes, which are the condensation products of squaric acid with electron rich substrates, are a family of compounds which have found wide application in the domain of photonics due to their unique properties, namely sharp and intense absorption within the visible to near-infrared range [18]. These same properties also turned them attractive for several biological applications, including as sensitizers for PDT [19]. As a consequence, structural modification of squaraine dyes become a very active area of research. Though a considerable number of different squaraine compounds has been developed envisioning their use as PDT sensitizers, both the *in vitro* and *in vivo* evaluation of their photodynamic capacity has been poorly addressed [20–34].

Aminosquaraines, a particular class of cationic squaraine dyes bearing an amino group replacing one of the oxygens atoms of the central four member ring, have recently been shown to possess photodynamic activity against several human tumor cell lines [35,36]. Aminosquaraines are envisioned to possess some potential advantages over the common zwitterionic counterparts as their cationic character may facilitate cellular uptake, benefiting from the cell's membrane potential, while, at the same time, the amino group may conveniently favor the interaction with the biological medium. Moreover, besides the electron-donating character of the amino auxchromes red-shifts dye's absorption [37,38], the presence of the amino group on the squaric ring may imparts a certain degree of additional rigidification to the molecule's structure. This can diminish the non-radiative decay by photoisomerization leading to an inherent increase of the intersystem crossing efficiency from the singlet to the triplet state of the sensitizer, and, ultimately, of the efficiency of singlet oxygen generation.

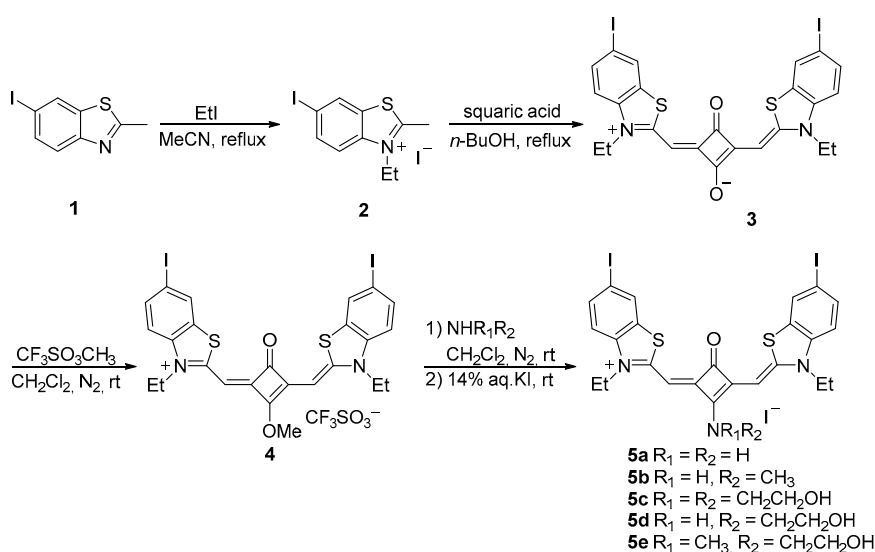
Herein we describe the synthesis of several new symmetrical diiodinated aminosquaraines and the evaluation of their singlet oxygen generation ability and photocytotoxicity against selected human tumor cell lines.

2. Results and Discussion

2.1. Synthesis of Dyes

The molecular design rationale of the aminosquaraines synthesized was driven by the attempt to amend molecule's rigidity, which influences the singlet oxygen production ability, dye's maximum absorption, which depends on the electron-donating characteristics of the amine auxochrome, and the ability to establish intermolecular hydrogen bonds, which may increase water solubility and provide a potential means for interaction with biological substrates. Therefore, the strategy consisted in selecting substituent groups able to generate secondary and tertiary amines, some of which possessing flexible hydroxyethyl arms.

Aminosquaraines **5a–e** were prepared by an expeditious synthetic method developed earlier by some of us [37], based on the methylation of one of the oxygen atoms of the squaraine core followed by nucleophilic substitution of the so-formed methoxy group by appropriate amines (Scheme 1).



Scheme 1. Synthesis of squaraine dyes **5a–e**.

Thus, condensation of two molar equivalents of benzothiazolium salt **2**, easily prepared by *N*-alkylation of 6-iodo-2-methylbenzothiazole (**1**) with iodoethane, with one equivalent of squaric acid in refluxing *n*-butanol/pyridine, resulted in the starting zwitterionic squaraine **3**. Methylation of the latter with methyl trifluoromethanesulfonate produced the crucial *O*-methyl ether derivative **4** from which the triflate analogues of **5a–e** could be obtained by treatment with the appropriate amines. Counter-ion exchange by iodine by treatment of the methanolic solutions of the dyes with excess 14% aqueous KI, produced the final aminosquaraine iodides **5a–e** in rather good yields. The counter ion exchange by iodine is carried out to potentially increase singlet oxygen generation through the external heavy atom effect [39]. As previously observed for several aminosquaraine dyes bearing a secondary amino group in the squaric ring [37,38], the two methylene protons of the polymethylene chain of **5b** and **5d** appear in the ¹H-NMR spectrum as separated signals as consequence of the consequent local magnetic field inhomogeneity, resulting from the intramolecular hydrogen bonding and/or hindered rotation around the C–N bond linking the amino substituent to the squaric ring.

2.2. Photochemical Characterization

2.2.1. UV-Visible Absorption Spectroscopy

All synthesized aminosquaraines **5a–e** display sharp and strong absorption in the red end of the visible spectrum, within the phototherapeutic window (Figure 1, Table 1). The absorption of dyes

5a–e is shifted bathochromically in relation to the non-substituted zwitterionic squaraine precursor **3**. The observed shifts ranging from 1 to 22 nm. The extent of the bathochromic shifts depends, in a direct way, on the electron donating ability of the amino auxochrome. This typical donor-acceptor mechanism is an usual feature of the chromophoric system of this class of compounds [37,38,40].

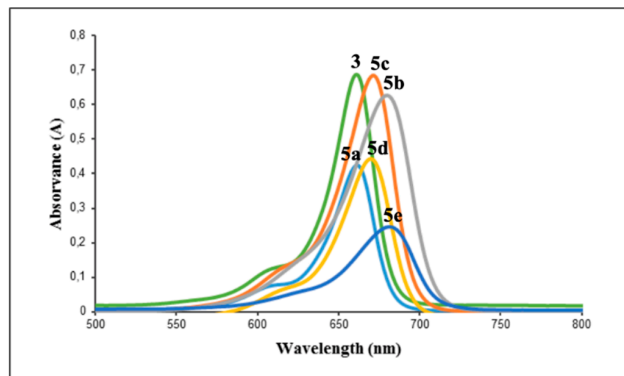


Figure 1. Absorption spectra of unsubstituted squaraine **3** and aminosquaraines **5a–e** in MeOH/CH₂Cl₂, 99/1 (*v/v*).

Table 1. Visible spectral data and fluorescence and singlet oxygen generation quantum yields of squaraine dyes **3** and **5a–e**.

Dye	R ₁	R ₂	λ _{max} ^a (nm)	log ε _{max} ^a	Φ _F ^b	Φ _Δ ^b
3	-	-	660	4.85	0.03	0.05
5a	H	H	661	5.40	0.02	0.22
5b	H	CH ₃	670	4.96	0.03	0.26
5c	CH ₂ CH ₂ OH	CH ₂ CH ₂ OH	679	4.91	0.01	0.09
5d	H	CH ₂ CH ₂ OH	671	5.04	0.11	0.19
5e	CH ₃	CH ₂ CH ₂ OH	682	4.50	0.09	0.16

^a In MeOH/CH₂Cl₂, 99/1 (*v/v*); ^b In CHCl₃.

2.2.2. Singlet Oxygen Quantum Yields

The evaluation of the photosensitizing efficiency of the aminosquaraine dyes was performed in chloroform, by determining the singlet oxygen formation quantum yields (Φ_Δ). Phenazine was used as standard [41,42]. The phosphorescence emission of singlet oxygen generated by the sensitizers at approximately 1270 nm is presented in Figure 2 and the determined quantum yields are summarized in Table 1.

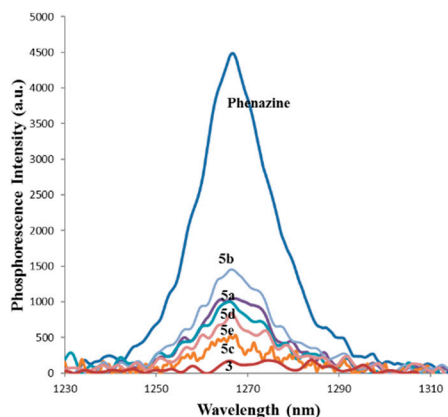


Figure 2. Singlet oxygen emission spectra of unsubstituted squaraine **3** and aminosquaraines **5a–e** in CHCl₃ against the reference compound (phenazine).

These Φ_{Δ} values were obtained by a simple comparison of the integrated areas determined for the standard and samples, using the same OD at the excitation wavelength. For each determination an average of 100 phosphorescence spectra were used. Dye **5b** displays the highest quantum yield when compared to the other squaraine derivatives ($\Phi_{\Delta} = 0.26$). As previously reported [43,44], the amino group in the squaric ring enhances singlet oxygen generation efficiency when compared with the unsubstituted zwitterionic dye **3**. The results for Φ_{Δ} are strongly dependent on the nature of the amino substituents: the highest Φ_{Δ} values occurred for the smallest substituents, and the lowest values were observed for the hydroxyethylamino substituents, especially the bis(hydroxyethyl)-amino group (dye **5c**). This is related with the intramolecular charge transfer (ICT) mechanism which provides a non-radiative deactivation pathway, therefore decreasing the singlet oxygen formation quantum yields ([44] and references therein).

2.2.3. Fluorescence Quantum Yields

Table 1 also presents the fluorescence quantum yields Φ_F for the aminosquaraines **5a–e** in CHCl_3 . As expected, due to the covalent link between iodine and the aminosquaraine, a strong heavy atom effect can be observed in all cases. This effect is emphasized in the case of the bis(hydroxyethyl)amino substituent group (dye **5c**).

2.3. In Vitro Photodynamic Activity

Four human tumor cell lines were used to assess the in vitro cytotoxicity of the synthesized dyes (**5a–e**): cervical (HeLa), breast (MCF7), hepatocellular (HepG2) and non-small cell lung (NCI-H460) carcinomas.

Although cytotoxicity was found to depend on the cell line, in general, all aminosquaraine dyes exhibited much higher cytotoxicity upon irradiation than in the absence of light. This fact revealed that the dyes are endowed with photodynamic action capacity. The assurance that the photodynamic effect was due, exclusively, to the sensitizing properties of the squaraine dyes, was secured by observing, in independent assays submitted to the photodynamic treatment and maintained in the dark, that, in the absence of the dyes neither DMSO nor light individually, nor the combination of both, were able to induce toxicity on the cells.

Figure 3 shows the growth inhibition ability of aminosquaraines **5a–e** against the different human tumor cell lines, in the absence of light and upon irradiation, at a dye concentration of $0.3 \mu\text{M}$. In this representative example, the growth inhibition in the dark was less than 20% in more than 75% of the assays.

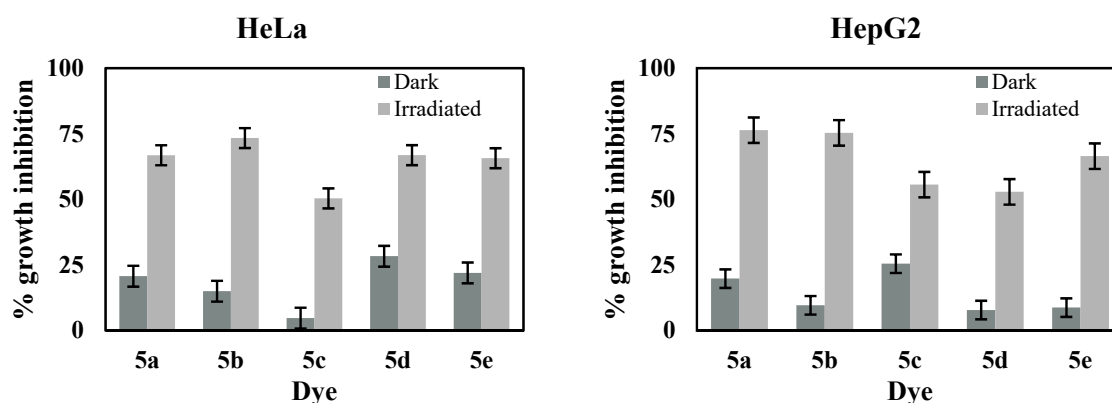


Figure 3. Cont.

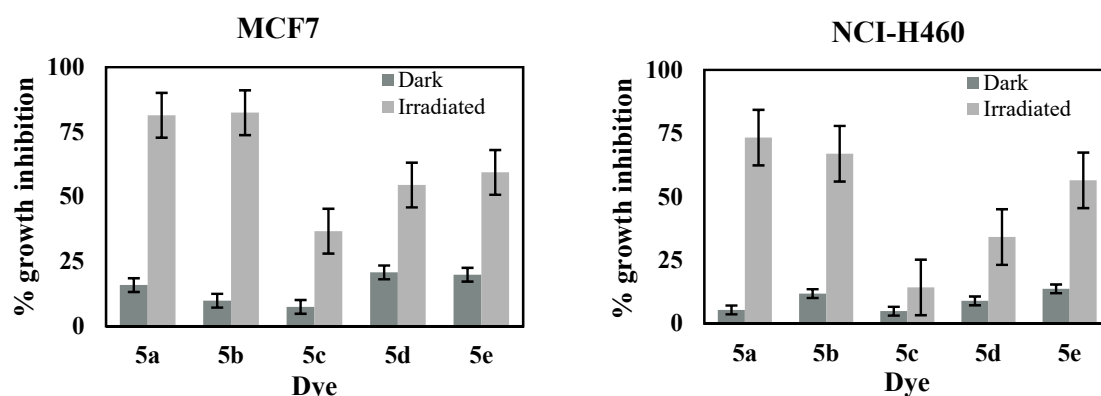


Figure 3. Growth inhibition of HeLa, HepG2, MCF-7 and NCI-H460 cell lines upon treatment with dyes **5a–e** ($0.3 \mu\text{M}$) in the dark and after irradiation. Results correspond to two independent assays and are presented as mean values \pm standard deviation (SD).

Whatever the cell line, dyes **5a** and **5b** exhibited, invariably, the larger differences between the growth inhibition percentages upon illumination and in the dark (~ 46 – 68% and ~ 43 – 73% , respectively). In case of dye **5a** the more pronounced differences in growth inhibition under the two conditions was found against the MCF-7 cell line, closely followed by the NCI-H460 cell line, while for dye **5b** the larger difference was observed for the MCF-7 cell line. Dye **5c** displayed the weaker photocytotoxic capability, presenting the smaller differences of growth inhibition in the presence and in the absence of light, for the HepG2, MCF-7 and NCI-H460 cell lines. For the HeLa cells dye **5d** showed to be the less efficient sensitizer. It is worthwhile to mention that, though determined in CHCl_3 , dye **5c** exhibited the lowest singlet oxygen generation quantum yield among all dyes tested.

The GI_{50} values (concentration causing 50% cell growth inhibition) for aminosquaraines **5a–e** were also determined and are presented in Table 2. The differences found between the values determined for the assays in the dark and upon irradiation, clearly demonstrated once more the photocytotoxic ability of the dyes.

Table 2. Cytotoxicity (GI_{50} values, μM) of aminosquaraine dyes **5a–e** (mean \pm SD).

Dye	Condition	HeLa	HepG2	MCF-7	NCI-H460	PLP2
5a	Dark	2.54 ± 0.02	20 ± 2	15 ± 1	15.3 ± 0.8	17.5 ± 0.1
	Irradiated	0.004 ± 0.0001	0.08 ± 0.001	0.01 ± 0.001	0.19 ± 0.02	2.0 ± 0.1
	<i>t</i> -Student test <i>p</i> -value	<0.001	<0.001	<0.001	<0.001	<0.001
5b	Dark	1.2 ± 0.1	15 ± 2	10.0 ± 0.7	8.1 ± 0.9	5.7 ± 0.6
	Irradiated	0.011 ± 0.01	0.06 ± 0.001	0.01 ± 0.001	0.18 ± 0.07	0.03 ± 0.001
	<i>t</i> -Student test <i>p</i> -value	<0.001	<0.001	<0.001	<0.001	<0.001
5c	Dark	2.0 ± 0.1	23 ± 2	>25	23 ± 2	22.0 ± 0.9
	Irradiated	0.31 ± 0.03	0.26 ± 0.03	0.42 ± 0.06	0.98 ± 0.04	0.44 ± 0.01
	<i>t</i> -Student test <i>p</i> -value	<0.001	<0.001	-	<0.001	<0.001
5d	Dark	1.8 ± 0.1	>25	>25	>25	>25
	Irradiated	0.19 ± 0.01	0.38 ± 0.03	0.25 ± 0.04	0.89 ± 0.01	0.98 ± 0.02
	<i>t</i> -Student test <i>p</i> -value	<0.001	-	-	-	-
5e	Dark	2.1 ± 0.2	11.4 ± 0.9	9.6 ± 0.2	13 ± 1	11.9 ± 0.2
	Irradiated	0.19 ± 0.02	0.19 ± 0.01	0.23 ± 0.02	0.24 ± 0.03	0.42 ± 0.01
	<i>t</i> -Student test <i>p</i> -value	<0.001	<0.001	<0.001	<0.001	<0.001

Among all compounds, **5a** and **5b** consistently presented the lowest GI_{50} values upon illumination for all the cell lines tested, ranging from $0.004 \mu\text{M}$ to $0.19 \mu\text{M}$. In the absence of light the GI_{50} values increased ca. 80–1500 times for **5a** and ca. 45–250 times for **5b**, depending on the cell line. With exception of the HeLa cells, dye **5d** showed to be inactive in the dark ($\text{GI}_{50} > 25 \mu\text{M}$) against all the cell lines within the range of the concentrations used.

One of the desirable features of any new sensitizer is the lack of toxicity for non-tumor cells. For that reason aminosquaraines **5a–e** were also tested against a non-tumor porcine liver primary cell culture (PLP2) established by some of us, both in the absence of light and under irradiation. Dye **5a** presented a GI_{50} value under illumination considerably superior to those determined for the tumor cell lines. Dyes **5b–d** displayed GI_{50} values against PLP2 cells, both in the dark and under irradiation, not appreciably different than those obtained for the tumor cell lines used.

Having recently demonstrated the photocytotoxic properties of several aminosquaraine dyes derived from benzothiazole [36], we anticipated that the introduction of iodine atoms in the terminal aromatic nucleus of the dyes could increase singlet oxygen generation through the heavy atom effect and, ultimately, enhance their photocytotoxicity. In fact, the GI_{50} values obtained for dyes **5a–e** under irradiation were in general smaller, in some cases substantially, than those determined previously for their non-halogenated analogues. The GI_{50} values in the dark, on the other hand, were higher, making aminosquaraines **5a–e** safer for application.

3. Materials and Methods

3.1. Chemistry

3.1.1. General Information

All reagents were obtained commercially and used as received. Solvents were of analytical grade. Anhydrous solvents were dried [45] and freshly distilled. All reactions were monitored by TLC using 0.20 mm aluminum-backed silica-gel plates (SIL G UV₂₅₄, Macherey-Nagel, Düren, Germany). Melting points were measured in a melting-point apparatus equipped with a binocular microscope (Rotoquímica, Maia, Portugal) and are uncorrected. IR spectra were recorded on a Unicam Research Series FT-IR spectrophotometer (Mattson Instruments Inc., Madison, WI, USA); ν_{\max} in cm^{-1} . Vis spectra were performed on a Lambda 25 instrument (Perkin-Elmer, Singapore); λ_{\max} in nm. ^1H - (400.13 MHz) and ^{13}C -NMR spectra (100.61 MHz) were recorded on an ARX 400 spectrometer (Bruker, Germany); δ in ppm relative to residual solvent signals, J in Hz. High resolution electrospray ionization time-of-flight mass spectra (HRMS ESI-TOF) were determined on Apex-Q FT-ICR and micrOTOF mass spectrometers (Bruker, Germany). 6-Iodo-2-methylbenzothiazole (**1**) was prepared as previously described [40].

3.1.2. Synthesis of 3-Ethyl-6-iodo-2-methylbenzothiazolium iodide (**2**)

A mixture of 6-iodo-2-methylbenzothiazole (**1**, 6.00 g, 22.00 mmol) and a 3-fold excess of iodoethane (5.40 mL, 66.00 mmol) in CH_3CN (150 mL) was heated under reflux for approximately 9 days. Upon cooling Et_2O was added and the resulting precipitate was collected by filtration under reduced pressure and washed with Et_2O . Yield: 68%. Yellowish crystals. M.p. > 265 °C (dec.).

3.1.3. Synthesis of 4-[(3-Ethyl-6-iodobenzothiazol-3-ium-2-yl)methylidene]-2-[(3-ethyl-6-iodo-3H-benzothiazol-2-ylidene)methyl]-3-oxocyclobut-1-en-1-olate (**3**)

A mixture of benzothiazolium salt **2** (2.00 g, 4.64 mmol) and squaric acid (0.27 g, 2.32 mmol) in *n*-BuOH/pyridine [9/1 (*v/v*)] (230 mL) was heated under reflux for about 4 h. The reaction mixture was then cooled in an ice bath, the resulting precipitate was collected by filtration under reduced pressure and washed thoroughly with water and Et_2O to afford chromatographically pure green crystals. Yield: 93%. M.p. > 300 °C. UV/Vis [$\text{MeOH}/\text{CH}_2\text{Cl}_2$, 99/1 (*v/v*)] λ_{\max} ($\log \epsilon$): 660 (4.85); ^1H -NMR ($\text{DMSO}-d_6$) δ : 8.22 (2H, s, ArH), 7.72 (2H, d, $J = 8.0$, ArH), 7.32 (2H, d, $J = 8.0$, ArH), 5.78 (2H, s, CH=C), 4.25 (4H, d, $J = 6.8$, NCH_2CH_3), 1.35–1.30 (6H, m, NCH_2CH_3). HRMS (ESI-TOF) m/z : 683.88936 ($[\text{M} - \text{I}]^+$, calc. for $\text{C}_{24}\text{H}_{20}\text{I}_2\text{N}_3\text{O}_2\text{S}_2$: 683.88761).

3.1.4. Synthesis of 3-Ethyl-2-[3-(3-ethyl-6-iodo-3*H*-benzothiazol-2-ylidenemethyl)-2-methoxy-4-oxocyclobut-2-enylidenemethyl]-6-iodobenzothiazol-3-ium trifluoromethanesulfonate (**4**)

To a solution of squaraine dye **3** (0.75 g, 1.10 mmol) in anhydrous CH₂Cl₂ (250 mL), stirred under N₂ atmosphere at r.t., was added an excess of CF₃SO₃CH₃ (1.0 mL, 8.80 mmol). After 22 h the reaction mixture was quenched with 5% (*m/v*) aqueous NaHCO₃ and the organic layer, after being separated by decantation, was dried over anhydrous Na₂SO₄. The solvent was then removed under reduced pressure to afford green crystals, which were found by TLC to have sufficient purity to be used in the next step without further purification. Yield: 89.6%. M.p. > 300 °C; UV/Vis [MeOH/CH₂Cl₂, 99/1 (*v/v*)] λ_{max} (log ε): 644 (5.34).

3.1.5. Synthesis of 2-[2-Amino-3-(3-ethyl-6-iodo-3*H*-benzothiazol-2-ylidenemethyl)-4-oxocyclobut-2-enylidenemethyl]-3-ethyl-6-iodobenzothiazol-3-ium iodide (**5a**)

To a solution of *O*-methylsquaraine **4** (0.30 g, 0.35 mmol) in anhydrous CH₂Cl₂ (125 mL), vigorously stirred under N₂ atmosphere at r.t., was added stepwise a 15.5-fold excess of a solution of 2 M NH₃ in MeOH. The reaction mixture was stirred at r.t. for 7 days. The resulting precipitate was collected by filtration under reduced pressure, washed with water and Et₂O and dissolved in MeOH. To this solution was added an approximately equal volume of 14% (*m/v*) aqueous KI. After stirring at r.t. for 1h, the precipitated dye was collected by filtration under reduced pressure and washed with water and Et₂O. Yield: 84%. Purple crystals. M.p. > 300 °C. UV/Vis [MeOH/CH₂Cl₂, 99/1 (*v/v*)] λ_{max} (log ε): 661 (5.40). ¹H-NMR (DMSO-*d*₆) δ: 8.53 (2H, s, NH₂), 8.34 (2H, s, ArH), 7.82 (2H, d, *J* = 8.0, ArH), 7.46 (2H, d, *J* = 8.6, ArH), 6.16 (2H, s, CH=C), 4.27 (4H, br q, *J* = 6.8, NCH₂CH₃), 1.35 (6H, br t, *J* = 6.6, NCH₂CH₃). ¹³C-NMR (DMSO-*d*₆) δ: 173.5, 165.7, 159.8, 157.5, 140.0, 136.0, 130.5, 129.7, 114.5, 88.0, 86.1, 41.3, 12.0. HRMS (ESI-TOF) *m/z*: 683.91317 ([M – I]⁺, calc. for C₂₄H₂₀I₂N₃OS₂: 683.91168).

3.1.6. Synthesis of 3-Ethyl-2-[3-(3-ethyl-6-iodo-3*H*-benzothiazol-2-ylidenemethyl)-2-(methylamino)-4-oxocyclobut-2-enylidenemethyl]-6-iodobenzothiazol-3-ium iodide (**5b**)

A mixture of *O*-methylsquaraine **4** (0.10 g, 0.12 mmol) and an excess of 2 M methylamine in MeOH (0.047 mL, 1.20 mmol), in anhydrous CH₂Cl₂ (125 mL), was stirred at r.t. under N₂ for about 2 days. The reaction mixture was then worked-up as above for **5a**. Yield: 70%. Purple crystals. M.p. > 300 °C. UV/Vis [MeOH/CH₂Cl₂, 99/1 (*v/v*)] λ_{max} (log ε): 671 (4.92). ¹H-NMR (DMSO-*d*₆) δ: 8.76 (1H, s, NHCH₃), 8.41 (1H, s, ArH), 8.35 (1H, s, ArH), 7.85–7.80 (2H, m, ArH), 7.52 (1H, d, *J* = 8.6, ArH), 7.46 (1H, d, *J* = 8.6, ArH), 6.17 (1H, s, CH=C), 6.05 (1H, s, CH=C), 4.38 (2H, br q, *J* = 7.3, NCH₂CH₃), 4.28 (2H, br q, *J* = 7.0, NCH₂CH₃), ~3.30 (NHCH₃, overlapped with residual HOD signal), 1.32–1.26 (6H, m, NCH₂CH₃). ¹³C-NMR (DMSO-*d*₆): 173.2, 164.1, 160.4, 159.0, 157.0, 156.4, 140.1, 140.0, 136.3, 136.0, 130.8, 130.5, 130.1, 130.0, 114.9, 114.6, 88.9, 88.3, 86.8, 86.2, 41.7, 41.1, 30.4, 12.3, 12.2. HRMS (ESI-TOF) *m/z*: 697.92882 ([M – I]⁺, calc. for C₂₅H₂₂I₂N₃OS₂: 697.92727).

3.1.7. Synthesis of 3-Ethyl-2-[3-(3-ethyl-6-iodo-3*H*-benzothiazol-2-ylidenemethyl)-2-[bis(2-hydroxyethyl)amino]-4-oxocyclobut-2-enylidenemethyl]-6-iodobenzothiazol-3-ium iodide (**5c**)

To a solution of *O*-methylsquaraine **4** (0.30 g, 0.35 mmol) in anhydrous CH₂Cl₂ (125 mL), under N₂ atmosphere, was added excess diethanolamine (0.084 mL, 0.89 mmol). After being stirred at r.t. for 9 days the reaction mixture was worked-up as above for **5a** and the resulting solid recrystallized from MeOH. Yield: 74%. Purple crystals. M.p. > 300 °C. UV/Vis [MeOH/CH₂Cl₂, 99/1 (*v/v*)] λ_{max} (log ε): 679 (4.91). ¹H-NMR (DMSO-*d*₆): 8.39 (2H, s, ArH), 7.83 (2H, d, *J* = 8.4, ArH), 7.50 (2H, d, *J* = 8.6, ArH), 6.09 (2H, s, CH=C), 5.17 (2H, s, NCH₂CH₂OH), 4.37 (4H, br s, NCH₂CH₃), 3.78 (8H, br s, NCH₂CH₂OH), 1.28 (6H, br s, NCH₂CH₃). ¹³C-NMR (DMSO-*d*₆): 173.5, 164.0, 159.2, 156.0, 140.0, 136.19, 130.6, 130.2, 114.8, 88.6, 87.9, 59.2, 53.7, 41.4 12.1. HRMS (ESI-TOF) *m/z*: 771.96560 ([M – I]⁺, calc. for C₂₈H₂₈I₂N₃O₃S₂: 771.96288).

3.1.8. Synthesis of 3-Ethyl-2-[3-(3-ethyl-6-iodo-3*H*-benzothiazol-2-ylidenemethyl)-2-[(2-hydroxyethyl)amino]-4-oxocyclobut-2-enylidenemethyl]-6-iodobenzothiazol-3-ium iodide (**5d**)

To a solution of *O*-methylsquaraine **4** (0.11 g, 0.13 mmol) in anhydrous CH₂Cl₂ (125 mL) and CH₃CN (60 mL), under N₂ atmosphere, was added excess ethanolamine (0.38 mL, 0.63 mmol). The reaction mixture was stirred at r.t. for about 5 days. The reaction mixture was worked-up as above for **5a**. Yield: 52%. Purplish blue crystals. M.p. > 300 °C. UV/Vis [MeOH/CH₂Cl₂, 99/1 (*v/v*)] λ_{max} (log ε): 670 (4.96). ¹H-NMR (DMSO-*d*₆): 8.90 (1H, s, NHCH₂CH₂OH), 8.39 (1H, s, ArH), 8.33 (1H, s, ArH) 7.84–7.78 (2H, m, ArH), 7.52–7.43 (2H, m, ArH), 6.29 (1H, s, CH=C), 5.95 (1H, s, CH=C), 5.13 (1H, s, NHCH₂CH₂OH), 4.35–4.28 (4H, m, NHCH₂CH₃), 3.74 (4H, br s, NHCH₂CH₂OH), 1.34–1.25 (6H, m, NCH₂CH₃). ¹³C-NMR (DMSO-*d*₆): 173.6, 163.9, 160.4, 158.9, 157.3, 156.0, 140.1, 140.0, 136.3, 136.1, 130.8, 130.5, 130.1, 114.9, 114.6, 88.9, 88.2, 87.2, 86.5, 60.5, 46.5, 41.7, 41.1, 12.4, 12.0. HRMS (ESI-TOF) *m/z*: 727.93938 ([M – I]⁺, calc. for C₂₆H₂₄I₂N₃O₂S₂: 727.93762).

3.1.9. Synthesis of 3-Ethyl-2-[3-(3-ethyl-6-iodo-3*H*-benzothiazol-2-ylidenemethyl)-2-[(2-hydroxyethyl)methylamino]-4-oxocyclobut-2-enylidenemethyl]-6-iodobenzothiazol-3-ium iodide (**5e**)

A mixture of *O*-methylsquaraine **4** (0.99 g, 0.12 mmol) and *N*-methylethanolamine (0.14 mL, 1.78 mmol) in anhydrous CH₂Cl₂ (125 mL) and CH₃CN (45 mL) was stirred at r.t., under N₂ atmosphere, for approximately 5 days. The precipitated solid was collected by filtration under reduced pressure and washed with water and Et₂O. The mother liquor was washed with water and the organic layer, after being separated by decantation, was dried over anhydrous Na₂SO₄ and evaporated to dryness under reduced pressure. The combined solids underwent counter ion exchange as described for **5a**. Yield: 56%. Blue crystals. M.p. > 300 °C. UV/Vis [MeOH/CH₂Cl₂, 99/1 (*v/v*)] λ_{max} (log ε): 682 (4.43). ¹H-NMR (DMSO-*d*₆): 8.39 (2H, s, ArH), 7.83 (2H, d, *J* = 8.6, ArH), 7.50 (2H, d, *J* = 8.8, ArH), 6.10 (2H, s, CH=C), 5.16 (1H, s, NCH₃CH₂CH₂OH), 4.39 (4H, s, NCH₂CH₃), 3.74 (4H, s, NCH₃CH₂CH₂OH), 3.48 (3H, s, NCH₃CH₂CH₂OH), 1.28 (6H, t, *J* = 5.5, NCH₂CH₃). HRMS (ESI-TOF) *m/z*: 741.95503 ([M – I]⁺, calc. for C₂₇H₂₆I₂N₃O₂S₂: 741.95297).

3.2. Photochemistry

Singlet Oxygen Quantum Yield Determinations

The singlet oxygen measurement set-up was assembled in our laboratory as previously described [43]. As an excitation source we used a nitrogen laser, excitation wavelength = 337 nm. The detector was an InGaAs CCD (model i-Dus from Andor Technology Limited, Belfast, UK) working at low temperature (−60 °C) coupled to a fixed spectrograph, model Shamrock 163i, also from Andor. Phenazine (standard) was used at O.D. = 0.6 in chloroform. The Φ_Δ values were obtained by comparing the total area of the emission spectra for the reference and for each dye under study in the same solvent, with the same optical density at the excitation wavelength. Phenazine (standard) was used at OD = 0.60 in CHCl₃.

3.3. Biology

3.3.1. General

Fetal bovine serum (FBS), L-glutamine, Hank's balanced salt solution (HBSS), trypsin-EDTA (ethylenediaminetetraacetic acid), penicillin/streptomycin solution (100 U/mL and 100 mg/mL, respectively), and RPMI-1640 were from Hyclone (Logan, UT, USA). Acetic acid, ellipticine, sulforhodamine B (SRB), trypan blue, trichloroacetic acid (TCA) and Tris were purchased from Sigma Chemical Co. (St. Louis, MO, USA). Water was treated in a Milli-Q water purification system (TGI Pure Water Systems, Greenville, SC, USA).

3.3.2. Preparation of the Solutions of Aminosquaraine Dyes

Stock solutions of the aminosquaraines **5a–e** with different concentrations (0.0375 μM , 0.15 μM , 0.6 μM , 6 μM , 12 μM , 25 μM , 50 μM , 500 μM) were prepared using a solution of 3% DMSO in DMEM and kept at $-20\text{ }^{\circ}\text{C}$. Prior to the in vitro assays diluted solutions were prepared with the same solvent to obtain solutions with final concentrations of 0.03 μM , 0.3 μM , 0.6 μM , 1.25 μM , 2.5 μM and 25 μM . For the HeLa MCF-7 cell lines solutions with final concentrations of 0.0075 μM and 0.001875 μM were additionally prepared once the inhibition percentage for the 0.03 μM solution was already superior to 50%.

3.3.3. Photodynamic Treatment

The cytotoxicity of the squaraine dyes was tested in the dark and under irradiation. For irradiation of the cells a halogen/tungsten lamp (24 V and 250 W, Osram, Carnaxide, Portugal) was used with a fluence rate of 23–24 $\mu\text{W}/\text{cm}^2$ (measured with an ILT 1400-A radiometer equipped with a SEL033 detector, ILT, Peabody, MA, USA). The cells were irradiated continuously for 30 min. A 3% aqueous solution of $\text{K}_2\text{Cr}_2\text{O}_7$ was placed between the lamp and the cells as a liquid cut off filter to remove light of wavelength shorter than $\sim 500\text{ nm}$. The temperature to which the cells were exposed was carefully monitored to guarantee cell viability.

3.3.4. Evaluation of Cytotoxicity in Human Tumor Cell Lines

Four human tumor cell lines were used: MCF-7 (breast adenocarcinoma), NCI-H460 (non-small cell lung carcinoma), HeLa (cervical carcinoma) and HepG2 (hepatocellular carcinoma) from DSMZ (Leibniz-Institut DSMZ-Deutsche Sammlung von Mikroorganismen und Zellkulturen GmbH, Mönchengladbach, Germany). Cells were routinely maintained as adherent cell cultures in RPMI-1640 medium containing 10% heat-inactivated FBS and 2 mM glutamine at $3\text{ }^{\circ}\text{C}$, in a humidified air incubator containing 5% CO_2 . Each cell line was plated at an appropriate density (7.5×10^3 cells/well for MCF-7 and NCI-H460, and 1.0×10^4 cells/well for HeLa and HepG2) in 96-well plates, allowed to attach for 24 h and then treated with different concentrations of each squaraine dye. Controls were set with the cells in the absence of the dyes in 3% DMSO in DMEM and in the growth medium only. After the incubation step (24 h), the cells were submitted to the photodynamic treatment for 30 min. Controls in the absence of light were performed on every test. Neither DMSO alone, nor light alone, nor the combination of both induced toxicity on the cells. Then, the growth medium was changed and the cells were incubated for further 24 h. Following this incubation period, the adherent cells were fixed by adding cold 10% TCA (100 μL) and incubated for 60 min at $4\text{ }^{\circ}\text{C}$. Plates were then washed with deionized water and subsequently dried. SRB solution (0.1% in 1% acetic acid, 100 μL) was then added to each plate well and incubated for 30 min at room temperature. Unbound SRB was removed by washing with 1% acetic acid. Plates were air dried, the bound SRB was solubilized with 10 mM Tris (200 μL) and the absorbance was measured at 540 nm in an ELX800 Microplate Reader (Bio-Tek Instruments Inc., Winooski, VT, USA) [46]. The results were expressed in GI_{50} values, which correspond to the concentration of dye that causes 50% inhibition of cell growth. All the assays were performed in duplicate. Ellipticine was used as standard.

3.3.5. Evaluation of Cytotoxicity in a Porcine Liver Primary Cell Culture

A cell culture was prepared from a freshly harvested porcine liver obtained from a local slaughter house, and it was designed as PLP2. Briefly, the liver tissues were rinsed in Hank's balanced salt solution containing 100 U/mL penicillin and 100 $\mu\text{g}/\text{mL}$ streptomycin and divided into $1 \times 1\text{ mm}^3$ explants to ensure that all liver cells were able to access the nutrients provided by the medium. Some of these explants were placed in 25 cm^2 tissue flasks in DMEM medium supplemented with 10% fetal bovine serum, 2 mM non-essential amino acids and 100 U/mL penicillin, 100 mg/mL streptomycin and incubated at $37\text{ }^{\circ}\text{C}$ with a humidified atmosphere containing 5% CO_2 . The medium was changed every two days. Cultivation of the cells was continued with direct monitoring every two or three

days using a phase contrast microscope. Before confluence was reached, cells were subcultured and plated in 96-well plates at a density of 1.0×10^4 cells/well, and cultivated in DMEM medium with 10% FBS, 100 U/mL penicillin and 100 μ g/mL streptomycin [47]. The PLP2 cells were incubated with the squaraine dyes and submitted to the two independent processes—dark and irradiation—as described earlier for the human tumor cell lines. The SRB assay was performed according to the procedure previously described. The results were expressed in GI₅₀ values. All the assays were performed in duplicate. Ellipticine was used as standard.

3.3.6. Statistical Analysis

All the assays were carried out in duplicate. The results are expressed as mean values and standard deviation. The results were analysed using a Student's *t*-test to determine the significant difference among the different samples, with $\alpha = 0.05$. This treatment was carried out using SPSS v. 22.0 program (IBM Corp., Armonk, NY, USA).

4. Conclusions

In conclusion, the synthesized aminosquaraine dyes, with strong absorption within the phototherapeutic window, showed photodynamic activity against the human tumor cell lines studied (MCF-7, NCI-H460, HeLa, and HepG2), inhibiting cell growth upon irradiation more than in the absence of light, in some cases substantially. When compared to the non-halogenated analogues dyes 5a–e exhibited, in general, lower GI₅₀ values under irradiation, which is probably related to the enhancement of singlet oxygen production through the so-called heavy atom effect. The difference of cytotoxicity observed in the dark and upon irradiation, turns some of the dyes potential candidates as photosensitizers for PDT, in particular compound 5a, which showed the lowest toxicity for the non-tumor primary PLP2 cells.

Author Contributions: Conceptualization, P.F.S.; Investigation, F.M., V.C.G., R.C.C., I.L.F.M. and L.F.V.F.; Supervision, I.C.F.R.F. and P.F.S.; Writing—original draft, F.M., L.F.V.F. and P.F.S.; Writing—review & editing, I.C.F.R.F. and P.F.S.

Funding: The authors are grateful to the Foundation for Science and Technology (FCT, Portugal) and FEDER for CMO (UID/AGR/00690/2013) and CQ-VR (UID/QUI/00616/2013) financial support, as also for R. Calhella contract.

Conflicts of Interest: The authors declare no conflict of interest.

References

1. Hamblin, M.R.; Mroz, P. *Advances in Photodynamic Therapy: Basic, Translational, and Clinical*; Artech House: Norwood, MA, USA, 2008.
2. van Straten, D.; Mashayekhi, D.; Bruijn, H.S.; Oliveira, S.; Robinson, D.J. Oncologic photodynamic therapy: Basic principles, current clinical status and future directions. *Cancers (Basel)* **2017**, *9*, 19. [[CrossRef](#)] [[PubMed](#)]
3. Henderson, B.W.; Dougherty, T.J. How does photodynamic therapy work? *Photochem. Photobiol.* **1992**, *55*, 145–157. [[CrossRef](#)] [[PubMed](#)]
4. Foote, C.S. Definition of type I and type II photosensitized oxidation. *Photochem. Photobiol.* **1991**, *54*, 659. [[CrossRef](#)] [[PubMed](#)]
5. Ochsner, M. Photophysical and photobiological processes in the photodynamic therapy of tumours. *J. Photochem. Photobiol. B* **1997**, *39*, 1–18. [[CrossRef](#)]
6. Niedre, M.; Patterson, M.S.; Wilson, B.C. Direct near-infrared luminescence detection of singlet oxygen generated by photodynamic therapy in cells in vitro and tissues in vivo. *Photochem. Photobiol.* **2002**, *75*, 382–391. [[CrossRef](#)]
7. Buytaert, E.; Dewaele, M.; Agostinis, P. Molecular effectors of multiple cell death pathways initiated by photodynamic therapy. *Biochim. Biophys. Acta* **2007**, *1776*, 86–107. [[CrossRef](#)] [[PubMed](#)]
8. Chen, B.; Pogue, B.W.; Hoopes, P.J.; Hasan, T. Vascular and cellular targeting for photodynamic therapy. *Crit. Rev. Eukaryot. Gene Expr.* **2006**, *16*, 279–305. [[CrossRef](#)]

9. Castano, A.P.; Mroz, P.; Hamblin, M.R. Photodynamic therapy and anti-tumor immunity. *Nat. Rev. Cancer* **2006**, *6*, 535–545. [[CrossRef](#)] [[PubMed](#)]
10. Hopper, C. Photodynamic therapy: A clinical reality in the treatment of cancer. *Lancet Oncol.* **2000**, *1*, 212–219. [[CrossRef](#)]
11. Bown, S.G. Photodynamic therapy for photochemists. *Philos. Trans. A Math. Phys. Eng. Sci.* **2013**, *371*, 1–16. [[CrossRef](#)] [[PubMed](#)]
12. O'Connor, A.E.; Gallagher, W.M.; Byrne, A.T. Porphyrin and nonporphyrin photosensitizers in oncology: Preclinical and clinical advances in photodynamic therapy. *Photochem. Photobiol.* **2009**, *85*, 1053–1074. [[CrossRef](#)] [[PubMed](#)]
13. Castano, A.P.; Demidova, T.N.; Hamblin, M.R. Mechanisms in photodynamic therapy: Part one-photosensitizers, photochemistry and cellular localization. *Photodiagnosis Photodyn. Ther.* **2004**, *1*, 279–293. [[CrossRef](#)]
14. Detty, M.R.; Gibson, S.L.; Wagner, S.J. Current clinical and preclinical photosensitizers for use in photodynamic therapy. *J. Med. Chem.* **2004**, *47*, 3897–3915. [[CrossRef](#)] [[PubMed](#)]
15. Abrahamse, H.; Hamblin, M.R. New photosensitizers for photodynamic therapy. *Biochem. J.* **2016**, *473*, 347–364. [[CrossRef](#)] [[PubMed](#)]
16. Ormond, A.B.; Freeman, H.S. Dye sensitizers for photodynamic therapy. *Materials* **2013**, *6*, 817–840. [[CrossRef](#)] [[PubMed](#)]
17. Dichiaro, M.; Prezzavento, O.; Marrazzo, A.; Pittalà, V.; Salerno, L.; Rescifina, A.; Amata, E. Recent advances in drug discovery of phototherapeutic non-porphyrinic anticancer agents. *Eur. J. Med. Chem.* **2017**, *142*, 459–485. [[CrossRef](#)] [[PubMed](#)]
18. Beverin, L.; Salice, P. Squaraine compounds: Tailored design and synthesis towards a variety of material science applications. *Eur. J. Org. Chem.* **2010**, *2010*, 1207–1225. [[CrossRef](#)]
19. Avirah, R.R.; Jayaram, D.T.; Adarsh, N.; Ramaiah, D. Squaraine dyes in PDT: From basic design to in vivo demonstration. *Org. Biomol. Chem.* **2012**, *10*, 911–920. [[CrossRef](#)] [[PubMed](#)]
20. Ramaiah, D.; Eckert, I.; Arun, K.T.; Weidenfeller, L.; Epe, B. Squaraine dyes for photodynamic therapy: Mechanism of cytotoxicity and DNA damage induced by halogenated squaraine dyes plus light (> 600 nm). *Photochem. Photobiol.* **2004**, *79*, 99–104. [[CrossRef](#)]
21. Serpe, L.; Ellena, S.; Barbero, N.; Foglietta, F.; Prandini, F.; Gallo, M.P.; Levi, R.; Barolo, C.; Canaparo, R.; Visentin, S. Squaraines bearing halogenated moieties as anticancer photosensitizers: Synthesis, characterization and biological evaluation. *Eur. J. Med. Chem.* **2016**, *113*, 187–197. [[CrossRef](#)] [[PubMed](#)]
22. Sun, C.-L.; Liao, Q.; Li, T.; Li, J.; Jiang, J.-Q.; Xu, Z.-Z.; Wang, X.-D.; Shen, R.; Bai, D.-C.; Wang, Q.; et al. Rational design of small indolic squaraine dyes with large two-photon absorption cross section. *Chem. Sci.* **2015**, *6*, 761–769. [[CrossRef](#)] [[PubMed](#)]
23. Soumya, M.S.; Shafeekh, K.M.; Das, S.; Abraham, A. Symmetrical diiodinated squaraine as an efficient photosensitizer for PDT applications: Evidence from photodynamic and toxicological aspects. *Chem. Biol. Interact.* **2014**, *222*, 44–49. [[CrossRef](#)] [[PubMed](#)]
24. Ahn, H.-Y.; Yao, S.; Wang, X.; Belfield, K.D. Near-infrared-emitting squaraine dyes with high 2PA cross-sections for multiphoton fluorescence imaging. *ACS Appl. Mater. Interfaces* **2012**, *4*, 2847–2854. [[CrossRef](#)] [[PubMed](#)]
25. Ferreira, D.P.; Conceição, D.S.; Fernandes, F.; Sousa, T.; Calhelha, R.C.; Ferreira, I.C.F.R.; Santos, P.F.; Ferreira, L.F.V. Characterization of a squaraine/chitosan system for photodynamic therapy of cancer. *J. Phys. Chem. B* **2016**, *120*, 1212–1220. [[CrossRef](#)] [[PubMed](#)]
26. Gao, F.P.; Lin, Y.X.; Li, L.L.; Liu, Y.; Mayerhöffer, U.; Spent, P.; Su, J.G.; Li, J.Y.; Würthner, F.; Wang, H. Supramolecular adducts of squaraine and protein for noninvasive tumour imaging and photothermal therapy in vivo. *Biomaterials* **2014**, *35*, 1004–1014. [[CrossRef](#)] [[PubMed](#)]
27. Jetty, R.; Bander, Y.P.; Daniele, M.A.; Hanor, D.; Hung, H.-I.; Ramshesh, V.; Duperreault, M.F.; Nieminen, A.-L.; Lemasters, J.J.; Foulger, S.H. Protein triggered fluorescence switching of near-infrared emitting nanoparticles for contrast-enhanced imaging. *J. Mater. Chem. B* **2013**, *1*, 4542–4554. [[CrossRef](#)]
28. Ramaiah, D.; Eckert, I.; Arun, K.T.; Weidenfeller, L.; Epe, B. Squaraine dyes for photodynamic therapy: Study of their cytotoxicity and genotoxicity in bacteria and mammalian cells. *Photochem. Photobiol.* **2002**, *76*, 672–677. [[CrossRef](#)]

29. Soumya, M.S.; Abraham, A. Preclinical evaluation of symmetrical diiodinated squaraine dye on experimental animal models. *J. Glycobiol. S* **2013**, *1*, 1–6.
30. Devi, D.G.; Cibir, T.R.; Ramaiah, D.; Abraham, A. Bis(3,5-diiodo-2,4,6-trihydroxyphenyl)squaraine: A novel candidate in photodynamic therapy for skin cancer models in vivo. *J. Photochem. Photobiol. B Biol.* **2008**, *92*, 153–159. [[CrossRef](#)] [[PubMed](#)]
31. Devi, D.G.; Cibir, T.R.; Abraham, A. Bis(3,5-diiodo-2,4,6-trihydroxyphenyl)squaraine photodynamic therapy induces in vivo tumor ablation by triggering cytochrome c dependent mitochondria mediated apoptosis. *Photodiagnosis Photodyn. Ther.* **2013**, *10*, 510–517. [[CrossRef](#)] [[PubMed](#)]
32. Wie, Y.; Hu, X.; Shen, L.; Jin, B.; Liu, X.; Tan, W.; Shangguan, D. Dicyanomethylene substituted benzothiazole squaraines: The efficiency of photodynamic therapy in vitro and in vivo. *EBioMedicine* **2017**, *23*, 25–33.
33. Soumya, M.S.; Gayathri, D.D.; Shafeekh, K.M.; Das, S.; Abraham, A. Photodynamic therapeutic efficacy of symmetrical diiodinated squaraine in vivo skin cancer models. *Photodiagnosis Photodyn. Ther.* **2017**, *18*, 302–309. [[CrossRef](#)] [[PubMed](#)]
34. Saneesh, B.P.S.; Manu, P.M.; Dhanya, T.J.; Tapas, P.; Meera, R.N.; Surendran, A.; Aneesh, K.A.; Vadakkancheril, S.J.; Ramaiah, D.; Nair, S.A.; et al. Bis(3,5-diiodo-2,4,6-trihydroxyphenyl)squaraine photodynamic therapy disrupts redox homeostasis and induce mitochondria-mediated apoptosis in human breast cancer cells. *Sci. Rep.* **2017**, *7*, 42126. [[CrossRef](#)] [[PubMed](#)]
35. Friães, S.; Silva, A.M.; Boto, R.E.; Ferreira, D.; Fernandes, J.R.; Souto, E.B.; Almeida, P.; Ferreira, L.F.V.; Reis, L.V. Synthesis, spectroscopic characterization and biological evaluation of unsymmetrical aminosquarylium cyanine dyes. *Bioorg. Med. Chem.* **2017**, *25*, 3803–3814.
36. Magalhães, Á.F.; Graça, V.C.; Calhelha, R.C.; Ferreira, I.C.F.R.; Santos, P.F. Aminosquaraines as potential photodynamic agents: Synthesis and evaluation of in vitro cytotoxicity. *Bioorganic Med. Chem. Lett.* **2017**, *27*, 4467–4470. [[CrossRef](#)] [[PubMed](#)]
37. Reis, L.V.; Serrano, J.P.C.; Almeida, P.; Santos, P.F. New synthetic approach to aminosquarylium cyanine dyes. *Synlett* **2002**, *10*, 1617–1620.
38. Reis, L.V.; Serrano, J.P.; Almeida, P.; Santos, P.F. The synthesis and characterization of novel, aza-substituted squarylium cyanine dyes. *Dyes Pigm.* **2009**, *81*, 197–202. [[CrossRef](#)]
39. Wardle, B. *Principles and Applications of Photochemistry*; John Wiley & Sons, Inc.: West Sussex, Chichester, UK, 2009.
40. Santos, P.F.; Reis, L.V.; Duarte, I.; Serrano, J.P.; Almeida, P.; Oliveira, A.S.; Ferreira, L.F.V. Synthesis and photochemical evaluation of iodinated squarylium cyanine dyes. *Helv. Chim. Acta.* **2005**, *88*, 1135–1143. [[CrossRef](#)]
41. Redmond, R.W.; Gamlin, J.N. A compilation of singlet oxygen yields from biologically relevant molecules. *Photochem. Photobiol.* **1999**, *70*, 391–475. [[CrossRef](#)] [[PubMed](#)]
42. Scaiano, J.C.; Redmond, R.W.; Mehta, B.; Arnason, J.T. Efficiency of the photoprocesses leading to singlet oxygen generation by α -terthienyl: Optical absorption, optoacoustic calorimetry and infrared luminescence studies. *Photochem. Photobiol.* **1990**, *52*, 655–659. [[CrossRef](#)] [[PubMed](#)]
43. Ferreira, D.P.; Conceição, D.S.; Ferreira, V.R.A.; Graça, V.C.; Santos, P.F.; Ferreira, L.F.V. Photochemical properties of squarylium cyanine dyes. *Photochem. Photobiol. Sci.* **2013**, *12*, 1948–1959. [[CrossRef](#)] [[PubMed](#)]
44. Conceição, D.S.; Ferreira, D.P.; Graça, V.C.; Silva, C.R.; Santos, P.F.; Ferreira, L.F.V. Photochemical studies of new benzothiazole and benzoselenazole-derived aminosquarylium dyes. *Tetrahedron* **2015**, *71*, 967–976. [[CrossRef](#)]
45. Perrin, D.D.; Armarego, W.L.F.; Perrin, D.R. *Purification of Laboratory Chemicals*, 2nd ed.; Pergamon: Oxford, UK, 1980.
46. Calhelha, R.C.; Ferreira, I.C.F.R.; Peixoto, D.; Abreu, R.M.V.; Vale-Silva, L.A.; Pinto, E.; Lima, R.T.; Alvelos, M.I.; Vasconcelos, M.H.; Queiroz, M.-J.R.P. Aminodi(hetero)arylamines in the thieno[3,2-b]pyridine series: Synthesis, effects in human tumor cells growth, cell cycle analysis, apoptosis and evaluation of toxicity using non-tumor cells. *Molecules* **2012**, *17*, 3834–3843. [[CrossRef](#)] [[PubMed](#)]

47. Abreu, R.M.V.; Ferreira, I.C.F.R.; Calhella, R.C.; Lima, R.T.; Vasconcelos, M.; Adegá, F.; Chaves, R.; Queiroz, M.-J.R.P. Anti-hepatocellular carcinoma activity using human HepG2 cells and hepatotoxicity of 6-substituted methyl 3-aminothieno[3,2-b]pyridine-2-carboxylate derivatives: In vitro evaluation, cell cycle analysis and QSAR studies. *Eur. J. Med. Chem.* **2011**, *46*, 5800–5806. [[CrossRef](#)] [[PubMed](#)]

Sample Availability: Samples of the compounds are not available from the authors.



© 2019 by the authors. Licensee MDPI, Basel, Switzerland. This article is an open access article distributed under the terms and conditions of the Creative Commons Attribution (CC BY) license (<http://creativecommons.org/licenses/by/4.0/>).